Diagnostic and Interventional Imaging (2019) **100**, 169—175

ORIGINAL ARTICLE /*Musculoskeletal imaging*

MRI detection of radiographically occult fractures of the hip and pelvis in the elderly: Comparison of T2-weighted Dixon sequence with T1-weighted and STIR sequences

B. Heynen, C. Tamigneaux, V. Pasoglou, J. Malghem, B. Vande Berg, T. Kirchgesner*

Department of Medical Imaging, Cliniques Universitaires Saint-Luc, Université Catholique de Louvain, Institut de Recherche Expérimentale et Clinique (IREC), 1200 Brussels, Belgium

KEYWORDS
Bone fracture;
Hip;
Pelvis;
MRI;
Dixon sequence

Abstract
Purpose: To compare the diagnostic performance of T2-weighted Dixon, T1-weighted and Short-Tau Inversion Recovery (STIR) MR images for the detection of radiographically occult fractures (ROF) of the hip and pelvis in elderly patients after low-energy trauma.
Materials and methods: A total of 22 patients older than 50 years with suspected ROF after low-energy trauma was prospectively included. There were 9 men and 13 women, with a mean age of 80.9 years ± 12.5 (SD) (range: 52—100 years). T2-weighted Dixon, T1-weighted and STIR MR images were analyzed by 3 independent radiologists blinded to the clinical data and the results of other imaging examinations. Readers separately assessed each series of images for the presence of fractures on a per bone analysis. Diagnostic performance of each reader was compared for Dixon and non-Dixon sequences using contingency tables and McNemar test. Interobserver agreement was evaluated according to the Fleiss-Cuzick's kappa statistics.
Results: The sensitivity of the Dixon sequence in the detection of ROF ranged from 90.9% (20/22; 95% CI: 70.8—98.9%) to 100% (22/22; 95% CI: 84.6—100%). The sensitivities of the non-Dixon sequences in the detection of ROF ranged from 95.5% (21/22; 95% CI: 77.2—99.9%) to 100% (22/22; 95% CI: 84.6—100%).

* Corresponding author. Cliniques universitaires Saint-Luc, Department of Medical Imaging, 10, avenue Hippocrate, 1200 Brussels, Belgium.
E-mail address: thomas.kirchgesner@uclouvain.be (T. Kirchgesner).

https://doi.org/10.1016/j.diii.2018.11.008

For each reader, there were no statistical differences between combined Dixon and combined non-Dixon images for the detection of ROF ($P = 0.12$, 0.99 and 0.99). Interobserver agreement with T2-weighted Dixon water-only images was significantly lower than that with the STIR sequence (0.70—0.79 vs. 0.87—0.93).

Conclusion: T2-weighted Dixon may be a second-rate alternative to T1-weighted and STIR sequences for the detection of ROF of the hip and pelvis in elderly patients.

The estimated number of low-energy hip fracture in elderly patients is expected to rise from 1.7 million in the 90s to 6.3 million in 2050 worldwide [1]. Plain radiography is the cornerstone imaging modality, but radiographically occult fracture (ROF) of the hip and pelvis, defined as a fracture not visible on radiographs, is observed in 2 to 14% of the patients after low-energy trauma [2—5]. Diagnosis of ROF is necessary as undetected or delayed detection of ROF of the hip and pelvis are associated with higher morbidity and mortality [6—8]. Magnetic resonance imaging (MRI) is considered as the imaging modality of choice to assess suspected hip and pelvic fractures [2,9—14].

The most common MRI protocols to detect hip and pelvic fractures include T1-weighted spin-echo (SE) sequence in the coronal plane along with Short-Tau Inversion Recovery (STIR) or T2-weighted fast SE sequences with fat suppression in the coronal and transverse planes [6,11,13]. Several authors suggested an abbreviated protocol to decrease the examination time for elderly patients using fat- and fluid-sensitive sequences in the coronal imaging plane only [2,5,6,15].

The Dixon technique based on the simultaneous acquisition of in-phase and opposed-phased images allows the production of fat-only (water-suppressed) and water-only (fat-suppressed) images by post-processing [16]. Previous studies have demonstrated that the water-only images allowed equivalent or better fat suppression than the usually performed fat-saturated and STIR sequences [16—20]. Recent studies suggested that T2-weighted Dixon fat-only images could replace the T1-weighted SE sequence for the detection of bone marrow metastasis [21] and sacroiliitis [22]. It may be thus assumed that the T2-weighted Dixon sequence might replace T1-weighted SE and STIR sequences for the detection of ROF.

The purpose of this study was to compare the diagnostic performance of T2-weighted Dixon, T1-weighted SE and STIR sequences for the detection of ROF of the hip and pelvis after low-energy trauma in elderly patients.

Materials and methods

Patients

The current prospective single-center study was approved by the institutional ethic committee of our institution, and informed consent was obtained from all patients. Patients older than 50 years who were admitted to the emergency room between August 2017 and February 2018 for suspicion of fracture of the hip or pelvis after low-energy trauma and had radiographic examinations that included antero-posterior radiographs of the pelvis and antero-posterior and oblique radiographs of the symptomatic hip were eligible for the study.

Radiographs were read by the on-duty radiology resident with 3- to 5-years of experience in medical imaging. Patients with diagnosis of recent fracture at radiographs and patients with normal/inconclusive radiographs and low clinical suspicion of fracture were excluded. Patients with high clinical suspicion of fracture and normal or non-conclusive radiographs underwent multiple detector computed tomography (MDCT) examination as it is the standard of care in our institution (IQon Spectral CT®, Philips). Standard acquisition parameters of the MDCT were 120 kV/204 mAs and images were reconstructed with bone and soft tissue kernels.

After patients had undergone MDCT examination, two radiology residents responsible of the inclusion process asked the patients to freely participate to the study and further undergo MRI examination. Exclusion criteria were refusal to undergo MRI, contraindications to MRI, unavailability of the MRI examination and incomplete MRI examination (Fig. 1).

MR imaging parameters

MRI examinations were performed with a 3 T MR scanner (Magnetom Skyra®, Siemens Healthineers or Ingenia Achiva®, Philips). All MRI examinations involved both proximal femurs, iliac bones and sacrum with the standard MRI sequences used in our institution and a T2-weighted Dixon sequence specifically added for the purpose of the study. The standard MRI protocol included a T1-weighted turbo SE sequence in the coronal plane (repetition time (TR)/echo time (TE), 750/16 ms; field-of-view (FOV), 400 × 400; section thickness (ST), 4 mm; intersection gap (IG), 1 mm; length (L), 2 min 43 s) and a STIR sequence in the coronal plane (TR/TE, 11,697/60 ms; FOV, 400 × 400; ST, 4 mm; IG, 1 mm; L, 4 min 23 s) with a STIR sequence in the transverse plane. The coronal T2-weighted Dixon turbo SE sequence (TR/TE, 4940/80 ms; FOV, 400 × 400; ST, 4 mm; IG, 1 mm; L, 3 min 52 s) was added and randomly ordered in the MRI protocol. Coronal T1-weighted, STIR and T2-weighted Dixon

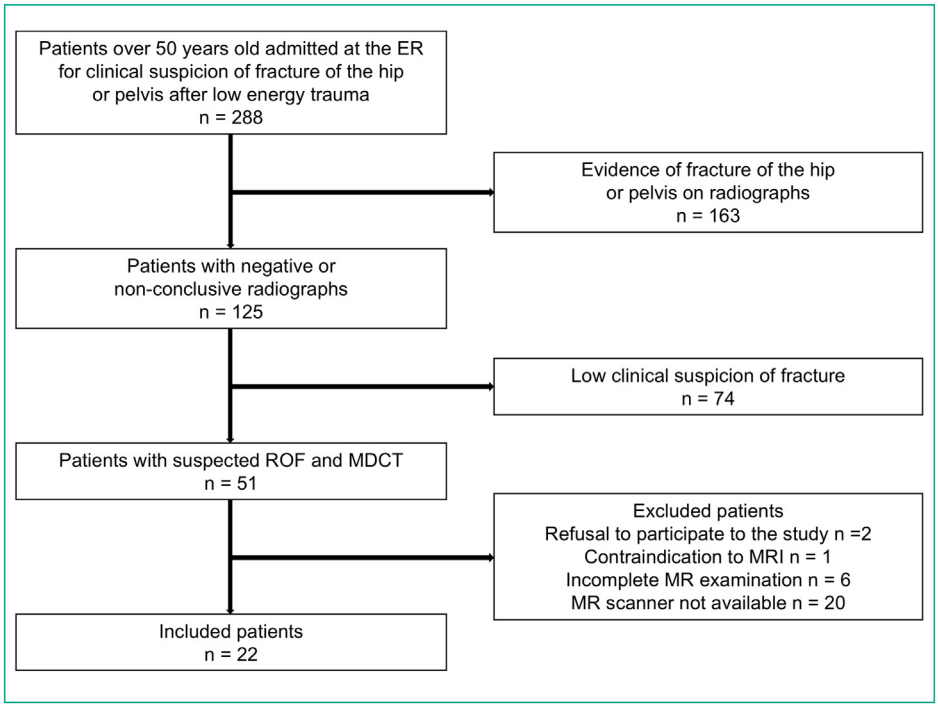

Figure 1. Flowchart demonstrating the inclusion process in the study.

fat- and water-only MR images were anonymized, randomly labelled and archived in our picture archiving and communication system (Carestream Vue 12.1.5.5151, Carestream Health, Inc.). T2-weighted Dixon in-phase and out-of-phase images were not used in the study.

Lesion definition

Bone fracture was defined as a poorly defined medullary area that demonstrated decreased signal intensity on fat-sensitive images (T1-and T2-weighted Dixon fat-only images) and high signal intensity on fluid-sensitive sequences (STIR and T2-weighted Dixon water-only images) with or without a linear component within the marrow changes (Fig. 2). The confidence level for the fracture was evaluated on a three-level Lickert scale: 1 indicated uncertainty; 2, a good degree of confidence; and 3, a high degree of confidence.

Image analysis

Between March and May 2018, one of the two last-year residents who had been involved in the inclusion process (B.H.) and two radiologists with 3 years of experience in musculoskeletal imaging (T.K. and V.P.) who had not been involved in the inclusion process analyzed the images for the presence or absence of bone fracture. Readers assessed separately bones and sequences blinded to all clinical information and all imaging data except the analyzed coronal MR images. Analysis of the images was performed on a per bone analysis to avoid the influence of the findings observed in the other bones when assessing the target bone. To do so, readers were asked to zoom the images and focus on the target bone only. After having analyzed the same bone of all patients in a given sequence, readers were asked to analyze another bone in the same sequence. Readers analyzed the bones in the following order: right femurs, left femurs, right pelvic bones, left pelvic bones and sacrums. After analysis of the 5 bones of all patients of the same sequence, readers assessed another series on a per bone analysis in a similar manner. Sequences were analyzed in the following order: T2-weighted Dixon fat-only, T1-weighted SE, Dixon water-only and STIR images.

The reference standard for the presence or absence of acute fracture was based on the retrospective analysis performed by a musculoskeletal radiologist (J.M.) with 35 years of experience in musculoskeletal imaging who had access to all medical and available imaging data including MDCT and MR images in the transverse plane.

Statistical analysis

The sensitivity, specificity and accuracy for each reader to detect fractures were calculated for each series of images and for combined Dixon and combined non-Dixon images using contingency tables along with their exact Clopper-Pearson 95% confidence intervals [23]. Results obtained with combined Dixon and combined non-Dixon images were compared using McNemar test. Statistically significant difference was set at $P < 0.05$. Lesions with a confidence level reading of 1 were considered negative for fracture and lesions with a confidence level reading of 2 or 3 were considered positive for fracture. In the combined analysis of fat- and fluid-sensitive series of images, fractures were considered positive if present in at least one of the two series. Interobserver agreement was evaluated for all bones in each series according to the Fleiss-Cuzick's kappa statistics. Agreement was interpreted as follows: Kappa ≤ 0.20

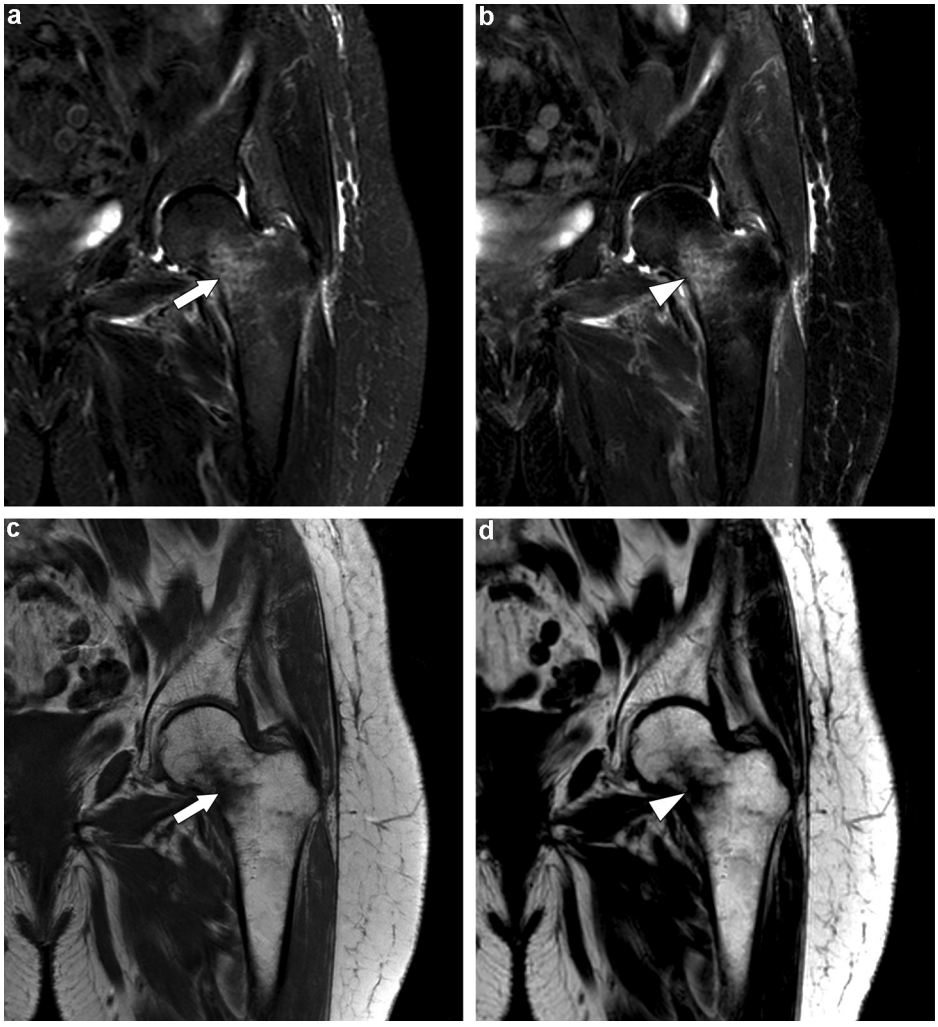

Figure 2. A 99-year-old woman with fracture of the left proximal femur after low-energy trauma. a: STIR image in the coronal plane reveals bone marrow edema with poorly defined high signal intensity of the bone marrow (arrow); b: T2-weighted Dixon water-only image demonstrates similar findings (arrowhead); c: T1-weighted SE image in the coronal plane also reveals bone marrow edema with poorly defined low signal intensity of the bone marrow (arrow); d: T2-weighted Dixon fat-only image demonstrates similar findings (arrowhead).

indicated poor agreement, Kappa between 0.21 and 0.40, fair agreement, Kappa between 0.41 and 0.60 moderate agreement, Kappa between 0.61 and 0.80 substantial agreement, and Kappa $\geq$ 0.81 very good agreement. Statistical analyses were conducted with the Medcalc software (Medcalc 18.5, Medcalc Statistical Software-Belgium).

Results

Study population

Between August 2017 and February 2018, 288 patients aged over 50 years were admitted at our emergency department because of pain and inability to walk after a low-energy trauma. Radiographs read by the on-duty radiology resident demonstrated recent fractures in 163 patients who were excluded from the study. Radiographs were considered to be negative or non-conclusive in 125 patients and MDCT was performed in 51 of them because of high clinical suspicion of ROF. After MDCT, 22 patients underwent further MRI examination within 24 hours after admission with the required sequences and were included in the study. There were 9 men and 13 women with a mean age of 80.9 years $\pm$ 12.5 (SD) (range: 50—100 years).

Among the included patients, 6 patients had no fractures and 16 patients had 22 fractures, including 3 femoral fractures, 12 pelvic bone fractures and 7 sacral fractures. Four femurs could not be assessed due to the presence of metal-related artifacts.

Comparison between Dixon and non-Dixon sequences

The sensitivity of the Dixon sequence in the detection of ROF ranged from 90.9% (20/22; 95% CI: 70.8—98.9%) to 100% (22/22; 95% CI: 84.6—100%). The sensitivities of the non-Dixon sequences in the detection of ROF ranged from 95.5% (21/22; 95% CI: 77.2—99.9%) to 100% (22/22; 95% CI: 84.6—100%). There were no statistical differences between combined Dixon and combined non-Dixon images for the detection of ROF for each reader (P = 0.12, 0.99, 0.99).

Table 1 Diagnostic performance to detect radiographically occult fractures of the hip and pelvis with combined Dixon and non-Dixon fat-and fluid-sensitive images in 22 patients.

Reader	Diagnostic performance	T2-weighted Dixon	T1-weighted SE + STIR
R1	Sensitivity	100 (22/22) [84.6—100]	100 (22/22) [84.6—100]
	Specificity	94.1 (79/84) [86.7—98.0]	98.8 (83/84) [93.5—100]
	Accuracy	95.3 (101/106) [89.3—98.5]	99.1 (105/106) [94.9—100]
R2	Sensitivity	95.5 (21/22) [77.2—99.9]	100 (22/22) [84.6—100]
	Specificity	95.2 (80/84) [88.3—98.7]	95.2 (80/84) [88.3—98.7]
	Accuracy	95.3 (101/106) [89.3—98.5]	96.2 (102/106) [90.6—99.0]
R3	Sensitivity	90.9 (20/22) [70.8—98.9]	95.5 (21/22) [77.2—99.9]
	Specificity	95.2 (80/84) [88.3—98.7]	94.1 (79/84) [86.7—98.0]
	Accuracy	94.3 (100/106) [88.1—97.9]	94.3 (100/106) [88.1—97.9]

Note. Numbers in parentheses are proportions. Numbers in brackets are 95% confidence intervals. SE indicates spin-echo.

Table 2 Diagnostic performance to detect radiographically occult fractures of the hip and pelvis with fat-sensitive Dixon and non-Dixon MR images in 22 patients.

Reader	Diagnostic performance	Dixon fat-only	T1-weighted SE
R1	Sensitivity	81.8 (18/22) [59.7—94.8]	90.9 (20/22) [70.8—98.9]
	Specificity	95.2 (80/84) [88.3—98.7]	100 (84/84) [95.7—100]
	Accuracy	92.5 (98/106) [85.7—96.7]	98.1 (104/106) [93.4—99.8]
R2	Sensitivity	90.9 (20/22) [70.8—98.9]	95.5 (21/22) [77.2—99.9]
	Specificity	96.4 (81/84) [89.9—99.3]	96.4 (81/84) [89.9—99.2]
	Accuracy	95.3 (101/106) [89.3—98.5]	96.2 (102/106) [90.6—99.0]
R3	Sensitivity	81.8 (18/22) [59.7—94.8]	86.4 (19/22) [65.1—97.1]
	Specificity	97.6 (82/84) [91.7—99.7]	94.1 (79/84) [86.7—98.0]
	Accuracy	94.3 (100/106) [88.1—97.9]	92.5 (98/106) [85.7—96.7]

Note. Numbers in parentheses are proportions. Numbers in brackets are 95% confidence intervals. SE indicates spin-echo.

Table 3 Diagnostic performance to detect radiographically occult fractures of the hip and pelvis with fluid-sensitive Dixon and STIR MR images in 22 patients.

Reader	Diagnostic performance	Dixon water-only	STIR
R1	Sensitivity	86.4 (19/22) [65.1—97.1]	95.5 (21/22) [77.2—100]
	Specificity	95.2 (80/84) [88.3—98.7]	98.8 (83/84) [93.5—100]
	Accuracy	93.4 (99/106) [86.9—97.3]	98.1 (104/106) [93.4—99.8]
R2	Sensitivity	90.9 (20/22) [70.8—98.9]	100 (22/22) [84.6—100]
	Specificity	97.6 (82/84) [91.7—99.7]	97.6 (82/84) [91.7—99.7]
	Accuracy	96.2 (102/106) [90.6—99.0]	98.1 (104/106) [93.4—99.8]
R3	Sensitivity	72.7 (16/22) [49.8—89.3]	86.4 (19/22) [65.1—97.1]
	Specificity	96.4 (81/84) [89.9—99.3]	98.8 (83/84) [93.5—100]
	Accuracy	91.5 (97/106) [84.5—96.0]	96.2 (102/106) [90.6—99.0]

Note. Numbers in parentheses are proportions. Numbers in brackets are 95% confidence intervals. STIR indicates short-tau inversion recovery.

Results are summarized in Table 1 for the comparison of combined fat- and fluid-sensitive sequences, Table 2 for the comparison of fat-sensitive sequences, Table 3 for the comparison of fluid-sensitive sequences and Table 4 for the comparison of the confidence level for the detection of fractures.

Interobserver agreement

The 2×2 interobserver agreement for the detection of fractures was substantial to very good for all sequences. Interobserver agreement was not statistically different between Dixon and non-Dixon fat-sensitive images

Table 4 Mean confidence level and standard deviation for the detection of radiographically occult fractures of the hip and pelvis of each reader with T2-weighted Dixon fat-only, T1-weighted SE, T2-weighted Dixon water-only and STIR images according to the gold standard of the study.

	Fracture	Fat-only	T1-weighted SE	Water-only	STIR
R1	Yes	2.32 ± 1.04	2.59 ± 0.85	2.59 ± 0.85	2.64 ± 0.79
	No	0.37 ± 0.58	0.17 ± 0.46	0.17 ± 0.46	0.12 ± 0.45
R2	Yes	2.68 ± 0.89	2.82 ± 0.66	2.82 ± 0.66	2.91 ± 0.29
	No	0.13 ± 0.53	0.10 ± 0.46	0.10 ± 0.46	0.07 ± 0.40
R3	Yes	1.91 ± 1.38	2.41 ± 1.14	2.41 ± 1.14	2.27 ± 1.20
	No	0.13 ± 0.58	0.19 ± 0.63	0.19 ± 0.63	0.14 ± 0.52

Note. Confidence level for fracture detection was scored as follow: 0: no fracture; 1: uncertainty; 2: good degree of confidence; and 3: high degree of confidence for the fracture. STIR indicates short-tau inversion recovery.

Table 5 Interobserver agreement with 2 × 2 comparison for the detection of radiographically occult fractures of the hip and pelvis with T2-weighted Dixon fat-only, T1-weighted SE, T2-weighted Dixon water-only and STIR MR images.

	Fat-only	T1 SE	Water-only	STIR
R1/R2	0.76 [0.69—0.83]	0.84 [0.79—0.89]	0.79 [0.73—0.85]	0.89 [0.85—0.93]
R2/R3	0.81 [0.75—0.87]	0.80 [0.74—0.86]	0.73 [0.66—0.80]	0.87 [0.82—0.92]
R1/R3	0.78 [0.71—0.85]	0.83 [0.78—0.88]	0.70 [0.63—0.80]	0.93 [0.90—0.96]

Note. Numbers in brackets are 95% confidence intervals. STIR indicates short-tau inversion recovery.

(0.76—0.81 for T2-weighted Dixon fat-only images and 0.80-0.84 for T1-weighted SE images). Interobserver agreement with T2-weighted Dixon water-only images was significantly lower than that with the STIR sequence (0.70—0.79 for T2-weighted Dixon water-only images and 0.87—0.93 for STIR images). Results for the interobserver agreement are summarized in Table 5.

Discussion

Our study demonstrated that T2-weighted Dixon MR sequence in the coronal plane has high diagnostic performance for the detection of occult fractures of the hip and pelvis in the elderly with confidence level similar to those of T1-weighted and STIR sequences in the coronal plane. However, the diagnostic performance of the T2-weighted Dixon sequence did not outreach those of the conventional sequences.

Our results concerning fat-sensitive images are in line with those of previous studies which demonstrated the potential of T1-weighted Dixon fat-only images as an alternative to the conventional T1-weighted SE sequence to detect bone metastases in patients with cancer [21] or to assess chronic signs of sacroiliitis [22]. On the contrary, our results with the fluid-sensitive images contrast with those of previous studies which demonstrated the superiority of the T2-weighted Dixon sequence in comparison with non-Dixon fluid-sensitive imaging [18,19,22]. Indeed, T2-weighted Dixon water-only images had lower sensitivity, accuracy and interobserver reproducibility than the STIR sequence in our study. In certain areas of the body, the Dixon technique may be less efficient than STIR sequence or chemical shift-selective (CHESS) technique as it has been recently demonstrated in the cervical spine [24]. It is possible that the benefit in terms of fat signal suppression and contrast-to-noise ratio with the T2-weighted Dixon water-only images does not yield any significant advantage in the detection of fracture when large field-of-views are used in which the STIR sequence also provides effective fat suppression with satisfying lesion depiction.

The T2-weighted Dixon sequence could be an alternative in a single sequence approach to the standard T1-weighted SE and STIR sequences in clinical practice. Indeed, reduced acquisition time of a single coronal T2-weighted Dixon sequence (less than 4 minutes for T2-weighted Dixon vs. 7 minutes for standard protocol) could increase the access to MRI for these patients during scheduled activities, especially using 2-point Dixon that is faster than the 3-point technique. Although it was not one of the objectives of our study, interestingly we noted that the coronal STIR sequence as a single sequence was excellent with an accuracy superior to that of all other sequences. These results are in accordance with those of Khurana et al. who suggested that a single coronal STIR sequence was sufficient to enable detection of radiographically occult fractures in elderly patients [15]. Moreover, the duration of the STIR sequence acquisition was similar to that of the T2-weighted Dixon in our study and could be reduced after further optimization [25]. This finding deserves further analysis as it was not within the scope of our study.

Our study had several limitations. First, this study was preliminary with a limited number of included patients and no power analysis was performed. We intentionally complexified the image analysis process to increase the number of analyzed bones and decrease the chance of a clustering

effect. Actually, the finding of a fracture interferes with the likelihood of another [26,27]. As an example, the presence of an obturator ring fracture increases the likelihood of a sacral fracture and decreases that of a femoral fracture. Second, readers did not analyze images obtained in the transverse plane as a single STIR sequence was obtained in this plane. We estimated that the MRI acquisition time would have been overlength with the addition of multiples sequences in the transverse plane. Anyway, the coronal plane has been demonstrated to be sufficient in this indication [15,25]. Third, we acknowledge that the combined analysis of fat- and fluid-sensitive images was artificial and based on separated single analysis. We deliberately separated the analysis of fat- and fluid-sensitive images to treat equally Dixon and non-Dixon sequences. However, Dixon sequences present a major benefit in clinical practice with the simultaneous production of fat- and fluid-sensitive images, which can be assessed together while two different non-Dixon sequences are necessary to do so.

In conclusion, our study demonstrates that T2-weighted Dixon fat- and water-only images may be a second-rate alternative to T1-weighted SE and STIR sequences in the detection of occult hip and pelvic fracture in elderly patients. However, our results also demonstrate the high diagnostic performance of a single coronal STIR sequence for this indication.

Disclosure of interest

The authors declare that they have no competing interest.

References

[1] Cooper C, Campion G, Melton LJ. Hip fractures in the elderly: a world-wide projection. Osteoporos Int 1992;2:285—9.

[2] Verbeeten KM, Hermann KL, Hasselqvist M, Lausten GS, Joergensen P, Jensen CM, et al. The advantages of MRI in the detection of occult hip fractures. Eur Radiol 2004;15:165—9.

[3] Dominguez S, Liu P, Roberts C, Mandell M, Richman PB. Prevalence of traumatic hip and pelvic fractures in patients with suspected hip fracture and negative initial standard radiographs — a study of emergency department patients. Acad Emerg Med 2005;12:366—9.

[4] Rizzo PF, Gould ES, Lyden JP, Asnis SE. Diagnosis of occult fractures about the hip. Magnetic resonance imaging compared with bone-scanning. J Bone Joint Surg Am 1993;75:395—401.

[5] Mandell JC, Weaver MJ, Khurana B. Computed tomography for occult fractures of the proximal femur, pelvis, and sacrum in clinical practice: single institution, dual-site experience. Emerg Radiol 2018;25:265—73.

[6] Kirby MW, Spritzer C. Radiographic detection of hip and pelvic fractures in the emergency department. AJR Am J Roentgenol 2010;194:1054—60.

[7] Leung WY, Ban CM, Lam JJ, Ip FK, Ko PS. Prognosis of acute pelvic fractures in elderly patients: retrospective study. Hong Kong Med J 2001;7:139—45.

[8] Ftouh S, Morga A, Swift C, Guideline Development G. Management of hip fracture in adults: summary of NICE guidance. BMJ 2011;342 [d3304].

[9] Berger PE, Ofstein RA, Jackson DW, Morrison DS, Silvino N, Amador R. MRI demonstration of radiographically occult fractures: what have we been missing? Radiographics 1989;9:407—36.

[10] Pandey R, McNally E, Ali A, Bulstrode C. The role of MRI in the diagnosis of occult hip fractures. Injury 1998;29:61—3.

[11] Cabarrus MC, Ambekar A, Lu Y, Link TM. MRI and CT of insufficiency fractures of the pelvis and the proximal femur. AJR Am J Roentgenol 2008;191:995—1001.

[12] Rehman H, Clement RG, Perks F, White TO. Imaging of occult hip fractures: CT or MRI? Injury 2016;47:1297—301.

[13] Collin D, Geijer M, Gothlin JH. Computed tomography compared to magnetic resonance imaging in occult or suspect hip fractures: a retrospective study in 44 patients. Eur Radiol 2016;26:3932—8.

[14] Haubro M, Stougaard C, Torfing T, Overgaard S. Sensitivity and specificity of CT- and MRI-scanning in evaluation of occult fracture of the proximal femur. Injury 2015;46:1557—61.

[15] Khurana B, Okanobo H, Ossiani M, Ledbetter S, Al Dulaimy K, Sodickson A. Abbreviated MRI for patients presenting to the emergency department with hip pain. AJR Am J Roentgenol 2012;198:W581—8.

[16] Guerini H, Omoumi P, Guichoux F, Vuillemin V, Morvan G, Zins M, et al. Fat suppression with Dixon techniques in musculoskeletal magnetic resonance imaging: a pictorial review. Semin Musculoskelet Radiol 2015;19:335—47.

[17] Del Grande F, Santini F, Herzka DA, Aro MR, Dean CW, Gold GE, et al. Fat-suppression techniques for 3-T MR imaging of the musculoskeletal system. Radiographics 2014;34:217—33.

[18] Brandao S, Seixas D, Ayres-Basto M, Castro S, Neto J, Martins C, et al. Comparing T1-weighted and T2-weighted three-point Dixon technique with conventional T1-weighted fat-saturation and short-tau inversion recovery (STIR) techniques for the study of the lumbar spine in a short-bore MRI machine. Clin Radiol 2013;68:e617—23.

[19] Kirchgesner T, Perlepe V, Michoux N, Larbi A, Vande Berg B. Fat suppression at 2D MR imaging of the hands: Dixon method versus CHESS technique and STIR sequence. Eur J Radiol 2017;89:40—6.

[20] Kirchgesner T, Perlepe V, Michoux N, Larbi A, Vande Berg B. Fat suppression at three-dimensional T1-weighted MR imaging of the hands: Dixon method versus CHESS technique. Diagn Interv Imaging 2018;99:23—8.

[21] Maeder Y, Dunet V, Richard R, Becce F, Omoumi P. Bone marrow metastases: T2-weighted Dixon spin-echo fat images can replace T1-weighted spin-echo images. Radiology 2018;286:948—59.

[22] Ozgen A. The value of the T2-weighted multipoint Dixon sequence in MRI of sacroiliac joints for the diagnosis of active and chronic sacroiliitis. AJR Am J Roentgenol 2017;208:603—8.

[23] Ahn S, Park SH, Lee KH. How to demonstrate similarity by using noninferiority and equivalence statistical testing in radiology research. Radiology 2013;267:328—38.

[24] Ross AB, Chan BY, Yi PH, Repplinger MD, Vanness DJ, Lee KS. Diagnostic accuracy of an abbreviated MRI protocol for detecting radiographically occult hip and pelvis fractures in the elderly. Skeletal Radiol 2018, http://dx.doi.org/10.1007/s00256-018-3004-7.

[25] Chiang IC, Chuang WS, Hang IT, Kuo YT, Hsieh TJ. Benefits and pitfalls of iterative decomposition of water and fat with echo asymmetry and least-squares estimation (IDEAL) imaging in clinical application of the cervical spine MR. Clin radiol 2018, http://dx.doi.org/10.1016/j.crad.09.002.

[26] Cosker TD, Ghandour A, Gupta SK, Tayton KJ. Pelvic ramus fractures in the elderly: 50 patients studied with MRI. Acta Orthop 2005;76:513—6.

[27] Collin D, Geijer M, Gothlin JH. Prevalence of exclusively and concomitant pelvic fractures at magnetic resonance imaging of suspect and occult hip fractures. Emerg Radiol 2016;23:17—21.